Civil Engineering and Applied Solutions

Research Article

journal homepage: ceas.journals.umz.ac.ir

CEAS Civil Engineering and Applied Solutions

Enhancing the Performance of High-Speed Railway Slab-Ballast Transition Zones Using Geotextile Reinforcement: A Dynamic-Equivalent 3D Finite Element Investigation

Nima Moslemi Patrudi [a*], Hossein Ghasemzadeh Tehrani [a], Iman Aghayan [a, b], Mohsen Bagheri [c]

[a] *Faculty of Civil Engineering, Shahrood University of Technology, Shahrood, Iran*
[b] *Department of Civil & Environmental Engineering, University of Wisconsin, Milwaukee, WI 53211, USA*
[c] *Faculty of Civil Engineering, Babol Noshirvani University of Technology, Babol, Iran*

ARTICLE INFO

Article history:

Received 29 May 2026

Revised 07 July 2026

Accepted 01 August 2026

Available online 01 April 2027

Keywords:

High-speed railway

Transition zone

Geotextile reinforcement

Finite element analysis

Nonlinear dynamic analysis

ABSTRACT

Transition zones between ballast and slab tracks are critical points in high-speed railways due to abrupt stiffness variations. This study investigates the optimization of speed-induced track responses in railway transition zones using geotextile reinforcement through a three-dimensional finite element dynamic-equivalent analysis. To address the inherent tensile weakness of the ballast layer, various geotextile lengths (6, 9, and 12 m) were modeled under heavy loading at speeds of 160 and 500 km/h. The numerical model was validated against experimental data of geosynthetic-stabilized soil under cyclic loading, showing a deviation of less than 10%. Results indicate that increasing train speed significantly intensifies rail deflection and impact coefficients. However, the inclusion of geotextile over cement-stabilized ballast enhances confinement and tensile strength, leading to a 60% reduction in vertical rail deformation compared to the unreinforced state. Among the tested configurations, a 12-meter geotextile length provided the optimal performance in reducing vertical rail displacement and smoothing the stiffness transition. These findings demonstrate that geotextile reinforcement is a highly effective and practical reinforcement strategy for enhancing the structural integrity and longevity of high-speed railway transition zones.

How to cite this article: Moslemi Patrudi, N., Ghasemzadeh Tehrani, H., Aghayan, I., Bagheri, M. Enhancing the Performance of High-Speed Railway Slab-Ballast Transition Zones Using Geotextile Reinforcement: A Dynamic-Equivalent 3D Finite Element Investigation. Civil Engineering and Applied Solutions. 2027; 3(2): 87–101. doi:10.22080/ceas.2026.31946.1105.

1. Introduction

High-speed railway (HSR) systems, characterized by operating speeds exceeding 160 km/h, have revolutionized modern transportation by demanding unprecedented levels of safety, passenger comfort, and structural precision. The operational integrity of these lines is highly sensitive to the dynamic interaction between the rolling stock and the trackbed, where any sudden variation in support conditions can compromise stability. A fundamental challenge in HSR infrastructure involves managing ‘transition zones’-critical interfaces where abrupt changes in vertical track stiffness occur, leading to magnified dynamic loads and accelerated structural degradation. Consequently, optimizing the mechanical response at these discontinuities is vital for ensuring the long-term reliability and efficiency of high-speed rail networks. The transition between flexible soil subgrades and rigid bridge abutments represents a critical discontinuity in railway tracks, primarily due to the sharp contrast in structural stiffness. Such disparities are a leading cause of geometric anomalies and uneven track settlement. Engineering practice dictates the use of specialized approach sections to harmonize these stiffness variations, providing a smoother mechanical transition and reducing the impact of differential

* Corresponding author.
E-mail addresses: moslemi_nima@shahroodut.ac.ir (N. Moslemi Patrudi).

https://doi.org/10.22080/ceas.2026.31946.1105
ISSN: 3092-7749/

settlement across the interface.

Shan et al. [1] studied the use of the Finite Element Method (FEM) to investigate the dynamic performance of two prevalent bridge-subgrade transition designs in high-speed railways: the two-part and the inverted trapezoid sections. Comparative analysis of track-subgrade displacement, acceleration, and surface stress reveals that the two-part transition zone exhibits superior dynamic stability. Furthermore, the results highlight a critical 3-meter zone from the bridge abutment where abrupt response changes occur, suggesting a minimum recommended transition length of 3 meters for enhanced structural integrity. Shih et al. [2] investigated the application of time-domain finite element (FE) models for representing moving loads on flexible railway tracks. Their systematic study compared various mesh geometries, boundary conditions, and soil damping models to provide comprehensive guidance for selecting appropriate FE parameters. They demonstrated that while infinite elements provide accuracy for harmonic loads, a sufficiently wide cuboid mesh combined with mass-proportional damping is more computationally efficient for moving load problems. Furthermore, they established that the model length required to achieve steady-state response significantly increases – up to 130 m – as the load approaches critical speeds in homogeneous grounds.

According to Chen and Zhou [3], the stiffness matching between high-rigidity fasteners and layered subgrade is essential for the dynamic stability of ballastless tracks. Using a 3D FEM model of the Beijing-Shanghai line, this study finds that while higher subgrade moduli reduce total displacement, fastener stiffness primarily impacts rail-level response. Notably, the modulus ratio between subgrade layers is identified as the dominant factor governing surface displacement under high-frequency loading. Connolly and Costa [4] identified a novel dynamic load amplification mechanism triggered by the interaction between vehicle axle configuration and the soil-guideway's vibration characteristics. Their numerical modeling, validated by field data, demonstrates that at speeds exceeding the critical velocity, load spacing sensitivity can increase displacements by up to 400%, significantly overshadowing the traditional critical velocity effects (50-100%). The study highlights the necessity of integrated vehicle-track design for future ultra-high-speed systems like Hyperloop and HSR to mitigate massive resonance effects. Zhou et al. [5] reviewed the key issues of subgrade settlement in high-speed railways built on soft soil, emphasizing that high compressibility and low permeability make post-construction settlement difficult to control and pose serious safety risks. They summarized theoretical and experimental foundation treatment methods for ballasted and ballastless tracks, discussed settlement evolution and control performance, and highlighted the limitations of existing prediction methods and the need for improved settlement control theories and technologies. Charoenwong et al. [6] proposed a novel numerical framework to predict track irregularity evolution by integrating empirical settlement laws with 3D finite element theory and multi-body vehicle-track interaction. Their study emphasizes the necessity of updating the track profile after every load passage to capture the evolving dynamic interaction accurately. The findings demonstrate that neglecting these progressive geometry changes leads to significant modeling errors and that subgrade material properties play a decisive role in long-term plastic settlement.

Wang et al. [7] investigated the mechanisms of railway heave in ballastless tracks induced by subgrade swelling in expansive soil regions. By integrating long-term longitudinal deformation monitoring, laboratory oedometer tests, and coupled FLAC3D-PFC3D numerical simulations, the authors identified that heave is a cumulative response to swelling in both subgrade filler and mudstone foundation layers. They established logistic functional relationships between swelling behavior and in-situ water content, while defining Expassoc and Nelder distribution models to quantify heave displacement based on swelling ratios. This research provides critical reference values for assessing swelling potential and predicting long-term deformations in similar geotechnical railway environments. Charoenwong et al. [8] conducted a comparative analysis of train-induced differential settlement between ballasted and concrete slab tracks at speeds of 200 km/h and 300 km/h. By developing a novel numerical model validated for both trackforms, the study demonstrates that ballasted tracks exhibit significantly higher rates of geometry deterioration compared to slab tracks, especially as line speeds increase. Their findings provide a scientific basis for trackform selection, highlighting that while slab tracks have higher initial costs, their superior resistance to differential settlement makes them more suitable for high-speed routes where maintenance windows are limited. Coelho et al. [9] investigated the transition zone near a concrete culvert, concluding that excessive dynamic displacements often stem from poor sleeper support rather than approach slab stiffness. Their field data also highlighted that ground motion and accelerations escalate as train speeds approach critical thresholds, necessitating enhanced support conditions in transition areas.

Sañudo et al. [10] at the University of Cantabria investigated the impact of train direction and pad positioning on the performance of track transition zones. Their study quantified the maximum vertical stresses and displacements within the ballast (beneath the sleepers) and under the main slab in ballastless track systems. By analyzing these peak responses, the research highlighted how the spatial configuration of track components and the direction of loading cycles significantly influence the stress distribution and long-term settlement at transition interfaces. Sadeghi et al. [11] employed nonlinear dynamic modeling to analyze the seismic response of road embankments, focusing on the role of soil liquefaction and PGA in driving permanent displacements. They evaluated how modifications to slope geometry and induced cracking compromise structural integrity, contributing to improved predictive assessments for the seismic durability of transportation infrastructure. Esen et al. [12] investigated the settlement behavior of a Geosynthetically Reinforced Soil with Retaining Wall (GRS-RW) railway system under static and cyclic loading conditions. A full-scale laboratory model including both concrete slab track and ballasted track was constructed on a 1.2 m subgrade with a frost protection layer. Results showed that the slab track exhibited significantly lower elastic and permanent deformations compared to the ballasted track, with about 25% lower rail displacement amplitude and 6-7 times smaller sleeper displacement under cyclic loading. These findings highlight the superior performance of slab track systems on GRS-RW foundations for railway applications. Jain et al. [13] investigated the persistent problem of degradation in railway transition zones by evaluating commonly used mitigation measures and proposing a new transition structure. The study first assessed traditional solutions, including horizontal and inclined approach slabs and transition wedges, using kinematic response, stress analysis, and an energy-based criterion based on total strain energy minimization. Subsequently, a newly proposed Safe Hull-Inspired Energy Limiting Design (SHIELD) was analyzed using the same evaluation criterion. The results of a two-dimensional finite element analysis indicated that the SHIELD concept effectively manages energy flow in transition zones and provides insight into the limitations of conventional transition structures. The study also demonstrated the robustness of the energy-based criterion and highlighted the potential of the SHIELD concept as a promising solution for improving the design of railway transition zones. Jain et al. [14] examined the challenges associated with railway transition zones caused by sudden stiffness variations and differential settlements when tracks pass over rigid structures such as bridges or culverts. The study evaluated the effectiveness of different sleeper configurations and reduced sleeper spacing in mitigating dynamic amplification in transition zones using a criterion based on the total strain energy in track-bed layers. A two-dimensional finite element model of an embankment-bridge transition was employed, and the effect of hanging sleepers resulting from loss of contact between sleepers and ballast was also investigated. The results indicated that although modifications in sleeper configuration and spacing can influence the track response, these measures alone are insufficient to completely eliminate transition zone effects. Li et al. [15] investigated the dynamic behavior of the vehicle-track system at subgrade-bridge transition zones in seasonal frozen regions, considering environmental temperature changes and wheel-rail irregularities. A coupled environment-vehicle-track-foundation model was developed and validated using monitoring data. The results showed that freeze-thaw cycles can cause frost heave and thaw settlement, leading to significant changes in track deformation and dynamic responses. Freeze-thaw effects and differential settlement were found to have a stronger impact on wheel-rail vertical forces than frost heave alone. Rail distortion near bridge abutments was also identified as a key factor increasing lateral vehicle vibrations in transition zones. Cui et al. [16] investigated the nonlinear interaction between vehicle-track dynamics and structural damage in ballastless tracks under uneven subgrade settlement. A nonlinear vehicle-track-subgrade interaction model including interlayer separation and concrete damage plasticity was developed. The results showed that subgrade settlement can significantly amplify vibrations and accelerate structural damage in ballastless tracks. Settlement wavelength and amplitude were identified as key factors influencing deformation and damage evolution. The study highlights the importance of controlling uneven settlement to ensure the safety and durability of high-speed railway track systems. Tutumluer et al. [17] reviewed the use of geosynthetics in transportation infrastructure such as roads, railways, and airfields. The study discusses the role of materials like geogrids, geotextiles, and geocells in improving subgrade restraint and stabilizing unbound aggregates. The findings highlight that geosynthetics enhance stiffness and load distribution through bearing capacity improvement and lateral restraint mechanisms. Overall, the research demonstrates their effectiveness in improving the performance and durability of transportation systems. Hasheminezhad et al. [18] examined the role of geosynthetics in improving the resilience and sustainability of geotechnical infrastructure. The study highlights that geosynthetics enhance load distribution, reduce deformation, and increase the durability of structures such as roads, embankments, and retaining systems. Their applications in drainage improvement, landslide recovery, and flood mitigation are also discussed. In addition, recent advances in geosynthetic technologies and their role in life cycle cost analysis are reviewed. The findings emphasize the importance of geosynthetics in developing resilient and sustainable infrastructure. Mohan and Nandan [19] investigated the use of pine-needle-based natural geotextiles as a sustainable solution for improving road infrastructure performance. The study showed that these geotextiles enhance load distribution, water retention, and subgrade stability while reducing environmental impacts compared to conventional materials. Mechanical, durability, and environmental tests, along with numerical modeling, were conducted to evaluate their performance. The results indicate that pine-needle geotextiles can improve the durability and lifespan of road pavements and provide a sustainable alternative for road construction. Mohan and Nandan [20] demonstrated that alkali-treated pine needle geotextile (TPNG) serves as an effective, sustainable reinforcement for pavement subgrades. Their research shows that TPNG significantly enhances load-bearing capacity, increasing the California Bearing Ratio (CBR) by up to 185% and improving shear strength by raising the internal friction angle from 22° to 35°. Furthermore, the material reduces pavement settlement by up to 50% under cyclic loading, offering a viable, eco-friendly solution for resilient infrastructure. Petriaev and Fedorenko [21] propose a nonlinear elastoplastic finite element (FEM) approach in Plaxis to model geogrid behavior, accounting for detailed geometry and rib thickness. By verifying the model against experimental data, the study demonstrates that linear elastic assumptions are insufficient for accurate analysis. This research effectively captures the geogrid's performance in both unconfined and soil-confined conditions, providing a more precise framework for predicting tensile stress-strain relationships. Ahmadi et al. [22] proposed a hybrid numerical framework combining DEM, FDM, and FEM to simulate the initial development of differential settlement in railway transition zones. The approach models granular ballast behavior, track structure response, and vehicle-track dynamic interaction simultaneously. Results show that the method can capture void formation beneath sleepers, redistribution of contact forces, and progressive track irregularities under repeated axle loads. The study highlights the importance of gradual stiffness transitions to reduce long-term track settlement and maintenance needs. Punetha and Nimbalkar [23] investigated the dynamic behavior of railway track-bridge transition zones under moving train loads using a three-dimensional finite element model validated with field data. The study analyzed mechanisms such as unsupported sleeper formation and stress variations within track substructure layers. Results indicate that train speed, axle load, and wheel motion significantly affect stresses, displacements, and sleeper-ballast gaps. The research also shows that geoinclusion reinforcement can improve performance and reduce differential settlement in critical transition zones. Asghari et al. [24] investigated the dynamic behavior of railway bridge-track transition zones considering the effects of approach slab length, thickness, and train speed using a three-dimensional FEM model. The results indicate that increasing train speed intensifies deformation in the transition zone. Increasing the thickness and length of the approach slab significantly reduces deformation and improves track performance. The study highlights the importance of proper transition zone design to mitigate stiffness changes and dynamic loads. Hassan et al. [25] investigated the dynamic performance of railway transition zones between rigid structures and embankments using a validated three-dimensional finite element model. A parametric analysis was conducted to evaluate the effects of approach slab geometry and wedge-shaped backfill on reducing dynamic impacts and differential settlement. Results indicate that increasing slab thickness and length significantly reduces rail displacement, with thickness having a stronger influence. The study also shows that wedge-shaped backfill improves stiffness transition and overall track performance under high-speed loading.

In recent years, geosynthetic reinforcement has become an effective solution for improving the performance of geotechnical systems subjected to dynamic loading, particularly in transportation infrastructure. Previous studies have employed analytical formulations, laboratory experiments, centrifuge testing, and three-dimensional finite element simulations to investigate the behavior of reinforced embankments, pile-supported systems, reinforced foundations, and load transfer platforms under moving and cyclic loads. These investigations consistently demonstrated that geotextiles and geogrids enhance stress distribution, improve lateral confinement, reduce permanent deformation and settlement, and increase the overall stability and serviceability of reinforced soil systems [26-36].

Despite the considerable body of research on railway transition zones, previous studies have predominantly focused on transition-zone geometry optimization, stiffness variation analysis, settlement prediction, moving-load modeling, and dynamic vehicle-track interaction. Although these investigations have significantly improved the understanding of transition-zone behavior, limited attention has been devoted to the combined application of geotextile reinforcement and cement-stabilized ballast as a practical solution for mitigating stiffness discontinuities in slab-ballast transition zones. Furthermore, the influence of geotextile reinforcement length on the mechanical performance of high-speed railway transitions has not been systematically quantified. Therefore, a clear research gap remains regarding the effectiveness of geotextile confinement mechanisms and their contribution to stiffness enhancement and displacement reduction under high-speed railway loading conditions.

To address this gap, the present study develops a comprehensive three-dimensional finite element model to investigate the behavior of geotextile-reinforced slab-ballast transition zones. The proposed approach incorporates geotextile layers within cement-stabilized ballast and systematically evaluates the performance of different reinforcement lengths (6, 9, and 12 m). The principal novelties of this research include: (I) the development of a detailed 3D finite element framework for geotextile-reinforced railway transition zones; (II) the investigation of geotextile confinement effects on ballast behavior and stress redistribution; (III) the evaluation of the optimal reinforcement length for minimizing rail deflection and track deformation; and (IV) the quantification of track stiffness enhancement achieved through geotextile inclusion. By applying quasi-static loading near the slab-ballast interface, the study provides new insights into the mechanisms governing stiffness transition and offers a practical design framework for improving the long-term performance and structural reliability of high-speed railway infrastructure.

2. Numerical simulation

The numerical analysis was performed using ABAQUS 2017 finite element software. To achieve a balance between computational efficiency and accuracy, the model was initially conceptualized in 3D and then refined to capture the critical dynamic responses of the transition zone.

2.1. Geometry and model components

The geometric configuration of the transition zone was developed in accordance with Instruction 301 (Technical Specifications for Railway Tracks) to ensure structural compliance (Fig. 1). The foundation of the model comprises an embankment modeled as a solid block with a length of 100 m, a height of 2.3 m, and a width of 7 m. Integrated into this system is a 50-m-long slab track section, characterized by a width of 3.6 m and a height of 0.5 m, which includes pre-defined recesses for precise sleeper placement (Table 1). To represent the flexible portion of the track, a ballast layer extending 47.4 m was incorporated with a total thickness of 50 cm. This thickness accounts for the mandatory 35-cm minimum clearance beneath the sleepers plus the sleeper height, while the top width of 3.4 m provides a 40-cm ballast shoulder to maintain lateral stability during high-speed operations.

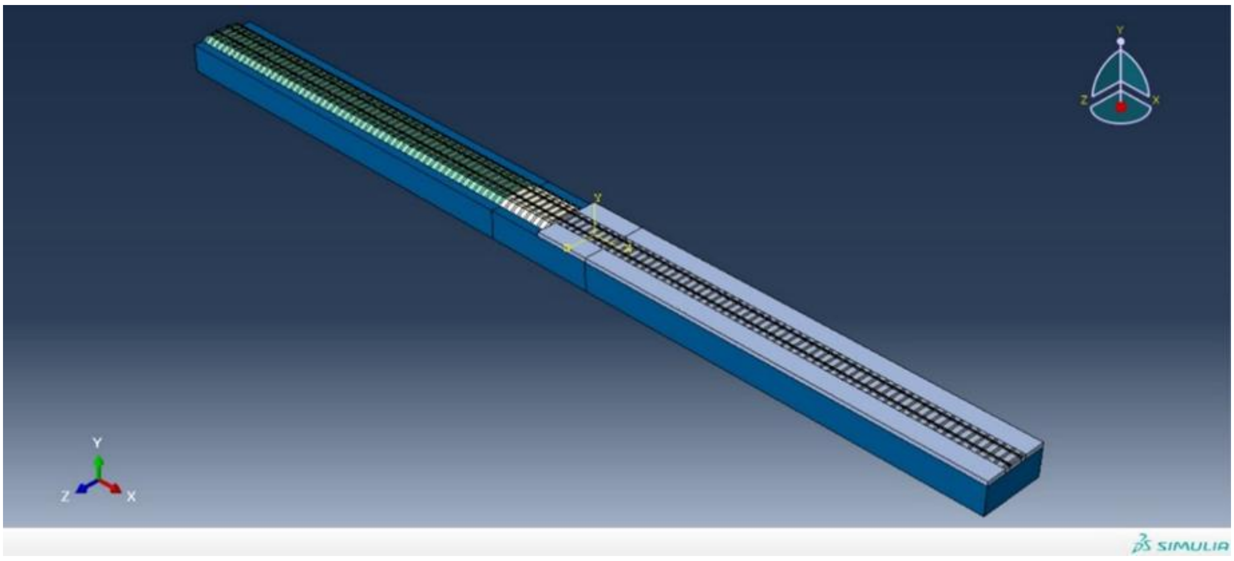

Fig. 1. General view of the 3D finite element model of the railway track system developed in Abaqus.

Table 1. Material properties used in the finite element model.

Model components	Density (kg/m^3)	Poisson's ratio	Modulus of elasticity (MPa)
Rail	7850	0.3	210000
Traverse	2500	0.2	29000
Ballast	1900	0.3	300
Railway embankment	1950	0.33	95
Element designed for cement-stabilized ballast	2500	0.2	25700
Slab track	3000	0.17	45000

The geotextile reinforcement was modeled using shell elements available in ABAQUS. A linear elastic constitutive model was adopted because the primary function of the geotextile in railway applications is to provide tensile reinforcement and lateral confinement, while its bending stiffness is generally negligible compared with the surrounding granular materials. The geotextile was therefore assumed to behave as a tension-resisting membrane with linear elastic properties throughout the analyzed loading range. The material properties were defined according to the manufacturer's technical specifications, including a tensile strength of 70 kN/m and a nominal thickness of 6.2 mm. Based on these parameters, the equivalent axial stiffness (EA) and corresponding elastic modulus were calculated and assigned to the shell elements. This modeling approach has been widely adopted in numerical studies of geosynthetic-reinforced transportation infrastructure and provides a reasonable representation of the reinforcement mechanism while maintaining computational efficiency.

Only one geotextile type was considered in the present study, and its mechanical properties were maintained constant in all simulations to isolate the influence of reinforcement length on transition-zone performance.

In the present study, the ballast layer was modeled as a linear elastic material to provide a consistent basis for comparing the relative effectiveness of different geotextile reinforcement lengths under identical modeling assumptions. This simplification was considered appropriate because the primary objective was to evaluate the comparative improvement in transition-zone performance rather than to reproduce the full nonlinear behavior of ballast materials. Nevertheless, it is recognized that railway ballast exhibits stress-dependent stiffness, irreversible plastic deformation, particle breakage, and rearrangement under repeated loading cycles, which are not explicitly captured in the current model.

The superstructure and reinforcement elements were modeled to capture the mechanical interactions at the interface. Concrete sleepers, with dimensions of 2.6 × 0.25 × 0.22 m (length × width × height), were positioned within the trackbed. The rail was represented by a rectangular section with an equivalent cross-sectional area of 0.0162 m^2, meticulously calibrated to match the moment of inertia and standard properties of a UIC 60 rail profile. Furthermore, the geosynthetic (geotextile) reinforcements were modeled as specialized elements designed to provide axial tensile strength and confinement (Table 2). These elements were specifically characterized by their zero bending stiffness, ensuring they resist only tensile forces to enhance the structural integrity of the ballast layer within the critical transition region.

Table 2. Characteristics of the applied geosynthetic material.

Name	Geotextile (800 g/m²)
Polymer type	PET
Unit weight (gr/m^2)	800
Thickness (mm)	6.2
Elongation in grab test	Over 50%
Wide-width tensile strength (kN/m)	70
Visible pore size (mm)	0.09
Permeability (cm/sec)	0.20

2.2. Interactions and boundary conditions

To simulate the physical connectivity of the track components, the rail-sleeper connections were modeled using linear springs to represent the rail pads and fastening systems. For the interfaces between the ballast/embankment and slab/subgrade, tie constraints were employed assuming no-slip conditions, justified by the quasi-static nature of the loading (Fig. 2). To optimize computational efficiency, the slab and sleeper components were merged, given their negligible relative displacement. Regarding the boundary conditions, the bottom surfaces were fully fixed in all directions, while the longitudinal ends were constrained to prevent any out-of-plane movement.

To minimize the influence of artificial boundary reflections, a total model length of 100 m was adopted based on recommendations reported in previous finite element studies of railway track systems. This length was considered sufficient to ensure that reflected stress waves do not significantly affect the response within the transition zone, which constitutes the primary region of interest. Nevertheless, it is acknowledged that advanced boundary treatments, such as infinite elements, viscous boundaries, or absorbing boundary conditions, may further reduce wave reflections in fully dynamic moving-load simulations. The implementation of such techniques is recommended for future investigations involving transient vehicle-track interaction analyses.

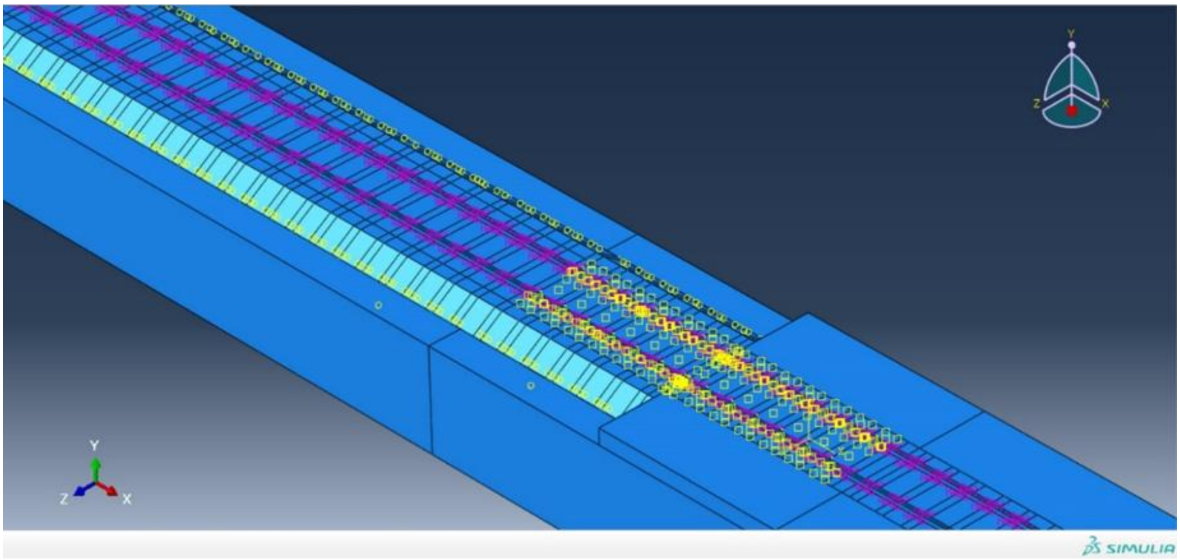

Fig. 2. Illustration of the interaction properties and boundary conditions assigned to the rail-sleeper and sleeper-ballast interfaces.

2.3. Loading and dynamic impact factor

The wheel loads were applied as quasi-static concentrated loads, incorporating dynamic effects at high speeds by multiplying the static wheel load (P_s) by a dynamic impact factor (φ), as Eq. 1.

$$P_d = \varphi . P_s \tag{1}$$

The impact factor was determined using a formula calibrated for the specific conditions of the Iranian railway network (Eq. 2).

$$\varphi = 1 + 4/73\frac{V}{D} \tag{2}$$

where V represents the train speed (km/h) and D is the wheel diameter (840 mm). Two distinct speed scenarios of 160 km/h and 500 km/h were analyzed, with loads strategically positioned 3 meters from the transition interface to accurately capture the peak vertical displacement (Table 3 and Fig. 3).

Table 3. Loading values of different train elements.

Train components	Load (N)
Locomotive body	1115000
Wagon body	940000
Three-axle bogie (locomotive)	180000
Two-axle bogie (wagon)	42000
Locomotive bogie axle	58000
Wagon bogie axle	18000
Total	2353000

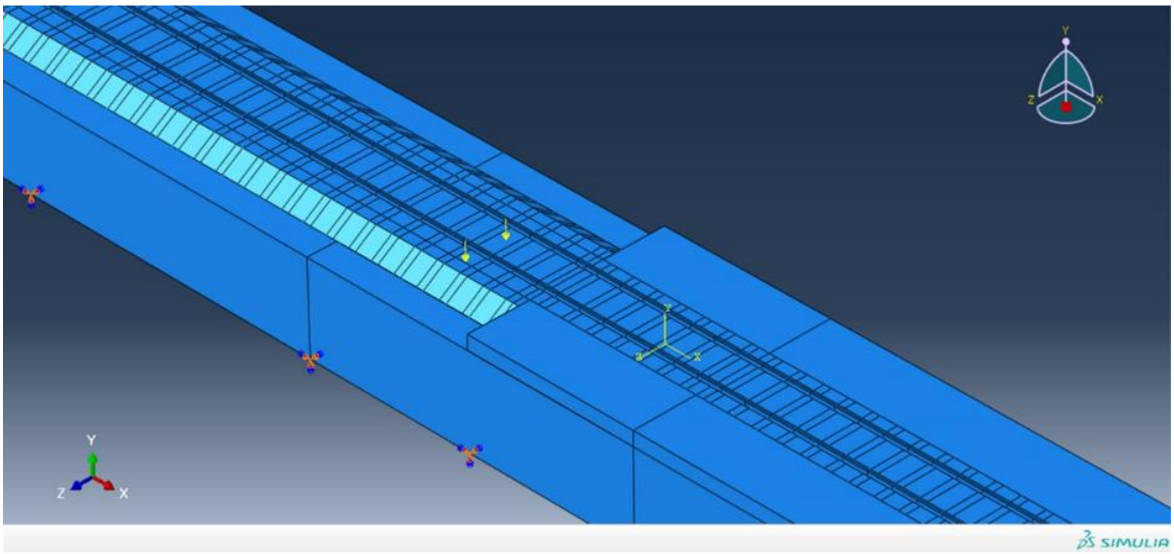

Fig. 3. Application of concentrated wheel loads on the rail surface for dynamic analysis and impact factor evaluation.

The Dynamic Impact Factor (DIF) adopted in this study was selected to account for the amplification of wheel loads induced by train speed and track irregularities. The employed formulation has been widely used in railway engineering practice and provides a simplified yet effective representation of speed-dependent dynamic loading effects. Although the adopted approach does not explicitly simulate moving wheel loads or vehicle-track interaction, it enables the incorporation of dynamic load amplification within a computationally efficient framework suitable for comparative parametric investigations of transition-zone performance. In addition to current high-speed railway operating conditions, a train speed of 500 km/h was considered as an upper-bound design scenario to evaluate the robustness of transition-zone performance under future ultra-high-speed railway systems. The inclusion of this speed does not imply current operational practice; rather, it reflects the growing interest in next-generation transportation technologies and the need to assess infrastructure performance beyond existing high-speed rail limits. As highlighted by Connolly and Costa (2020), the geodynamics of very-high-speed transport systems represent an emerging research area requiring the evaluation of track and subgrade behavior under increasingly demanding operational conditions. Accordingly, the 500 km/h scenario was adopted to investigate the resilience of the proposed geotextile-reinforced transition zone under extreme but plausible future loading conditions. The loading position was selected based on the findings of Shan et al. (2013), who reported that the region approximately 3 m away from the transition interface is where the most significant changes in response and peak displacements are observed. In addition, preliminary numerical analyses performed during the model development stage of this study also indicated that the maximum rail displacement occurs in the vicinity of this location. Therefore, the load was applied at this distance to capture the critical response behavior of the transition zone.

In this study, a dynamic-equivalent loading approach based on the Dynamic-Implicit formulation is adopted. Accordingly, explicit damping definitions such as Rayleigh damping are not introduced, as the response is governed by quasi-static equilibrium with inertia effects rather than full transient wave propagation. Nevertheless, it is recognized that energy dissipation mechanisms, including material and radiation damping, may influence the system response. These effects are therefore suggested to be incorporated in future studies for more comprehensive dynamic simulations. It should be noted that the present modeling framework does not represent a fully coupled vehicle-track dynamic interaction analysis. Instead, dynamic effects associated with train speed are incorporated through a Dynamic Impact Factor (DIF) applied to the static wheel loads. Therefore, the adopted methodology should be interpreted as a dynamic-equivalent analysis rather than a moving-load dynamic simulation. The adopted methodology represents a dynamic-equivalent analysis in which train-induced dynamic effects are incorporated through a Dynamic Impact Factor (DIF) rather than a fully coupled moving-load simulation. This simplified approach is commonly used in railway engineering studies to evaluate the influence of speed-dependent load amplification while maintaining computational efficiency.

The selected transition lengths of 6 m, 9 m, and 12 m were defined based on practical railway construction considerations. These values were chosen to represent short, medium, and extended reinforcement zones commonly implemented in transition-zone improvement practices. This range is consistent with typical design recommendations reported in railway engineering studies and allows for a comparative assessment of different reinforcement extents on system performance.

2.4. Solver and meshing

The Dynamic-Implicit solver was employed to ensure numerical convergence while accurately capturing time-dependent responses. The meshing strategy incorporated C3D8 (8-node linear brick) and C3D10 (10-node quadratic tetrahedron) elements for solid components, while S4 (4-node shell) elements were utilized for planar reinforcements. Furthermore, the mesh density was locally refined at the transition interface and beneath the loading points to enhance the accuracy of gradient calculations in these critical zones (Fig. 4).

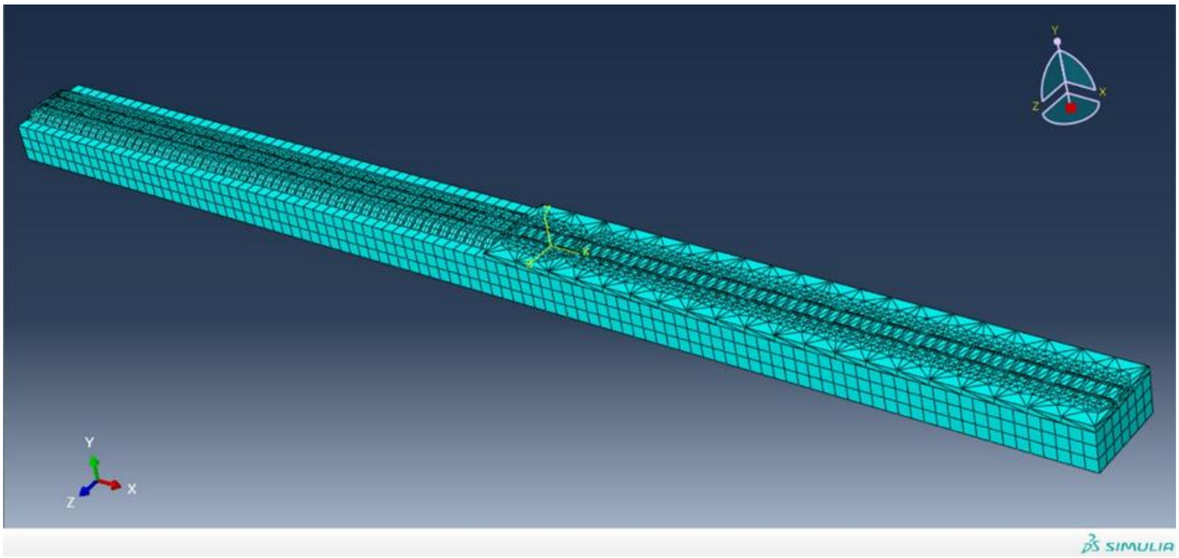

Fig. 4. Discretized finite element mesh of the 3D model with local mesh refinement in the zone of interest.

2.5. Mesh convergence study

To ensure that the numerical results are independent of mesh density, a mesh convergence study was performed. Three different mesh configurations were considered by progressively refining the mesh in the transition zone and beneath the loading area, where the highest stress and displacement gradients occur. The maximum vertical rail displacement was selected as the convergence criterion because it represents the primary response parameter used throughout the study. The results indicate that increasing the mesh density beyond the medium refinement level produced only marginal changes in the predicted rail displacement. The difference between the medium and fine meshes remained below 3%, demonstrating that the numerical solution had reached mesh independence. Therefore, the medium-fine mesh configuration was adopted for all subsequent analyses to achieve a suitable balance between computational efficiency and solution accuracy [37, 38].

2.6. Track bed stiffness

The track bed stiffness (K) is defined as the force required to produce a unit vertical displacement (Y), calculated as Eq. 3.

$$K = \frac{P_S}{Y} = \frac{P_S}{\sum_{m=0}^{m=\infty} Y_{n\pm m}} \tag{3}$$

This parameter serves as a key performance indicator (KPI) to evaluate the effectiveness of geotextile reinforcement in smoothing the stiffness transition between the ballasted track and the slab track sections.

The reported stiffness values in this study (Fig. 5) correspond to the equivalent track-bed stiffness, which is calculated using Eq. 3. This parameter accounts for the combined contribution of the track system components and is employed consistently throughout the numerical model to represent the stiffness condition of the railway structure.

3. Validation of the numerical model

To ensure the accuracy and reliability of the finite element simulations, the developed ABAQUS model was validated against the full-scale laboratory experimental results reported by Esen et al. [12]. Their study provides a comprehensive assessment of the immediate and long-term settlement behavior of GRS railway structures under cyclic loading for both slab track and ballasted track configurations. In the present study, the numerical framework was calibrated to replicate the experimental setup, material properties, and loading conditions of the reference study. The mean vertical displacement of the rail under static loading was extracted and compared with the experimental data from (Fig. 6). As summarized in Table 4, the maximum discrepancy between the numerical predictions and the experimental measurements remained below 10%. This high degree of correlation demonstrates the capability of the developed model to accurately capture the geomechanical response of the system, thereby justifying its use for further parametric investigations.

Although the agreement between the numerical predictions and the experimental measurements demonstrates the capability of the developed model to reproduce the observed rail displacement behavior, it should be noted that the validation was performed using vertical rail displacement as the primary response parameter. This selection was dictated by the availability of experimental data reported by Esen et al. [12], which mainly focused on displacement measurements. Additional validation using ballast stress distributions, permanent settlement accumulation, and field-monitoring data from railway transition zones would provide a more comprehensive assessment of model reliability and is recommended for future studies.

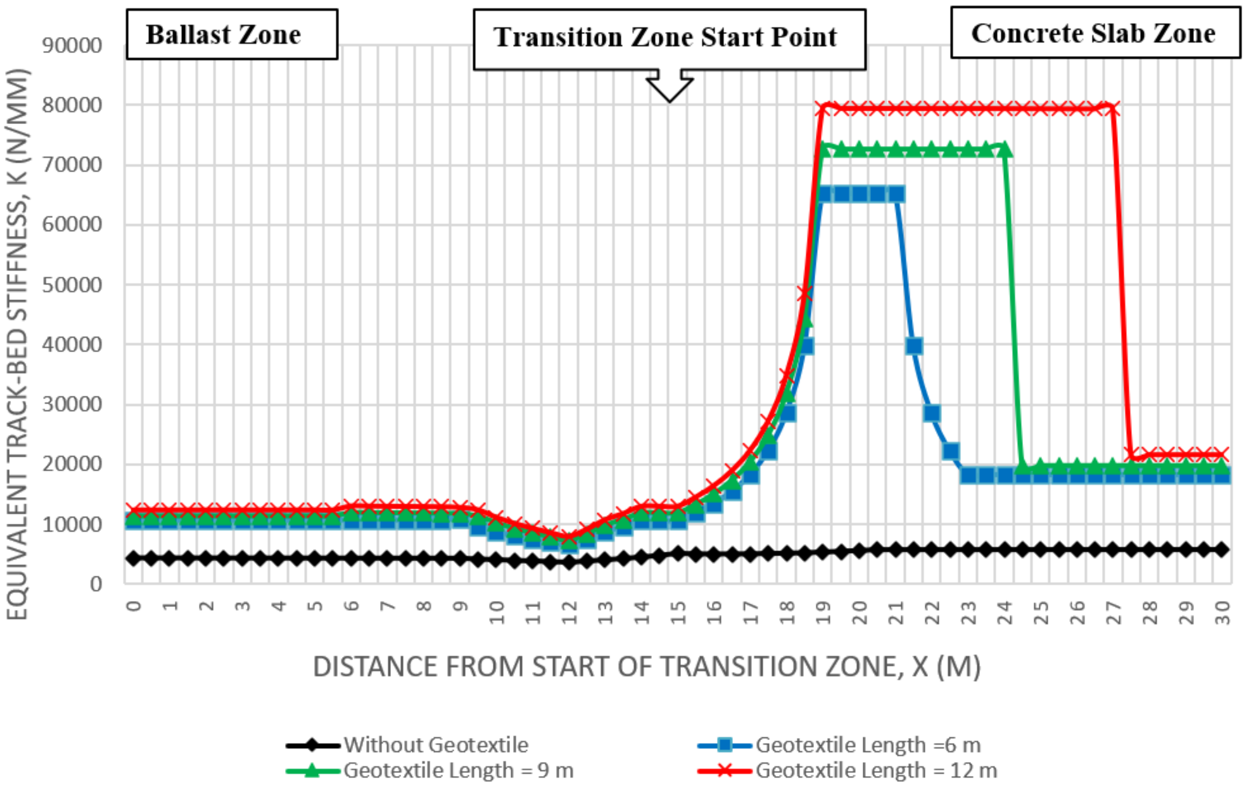

(a)

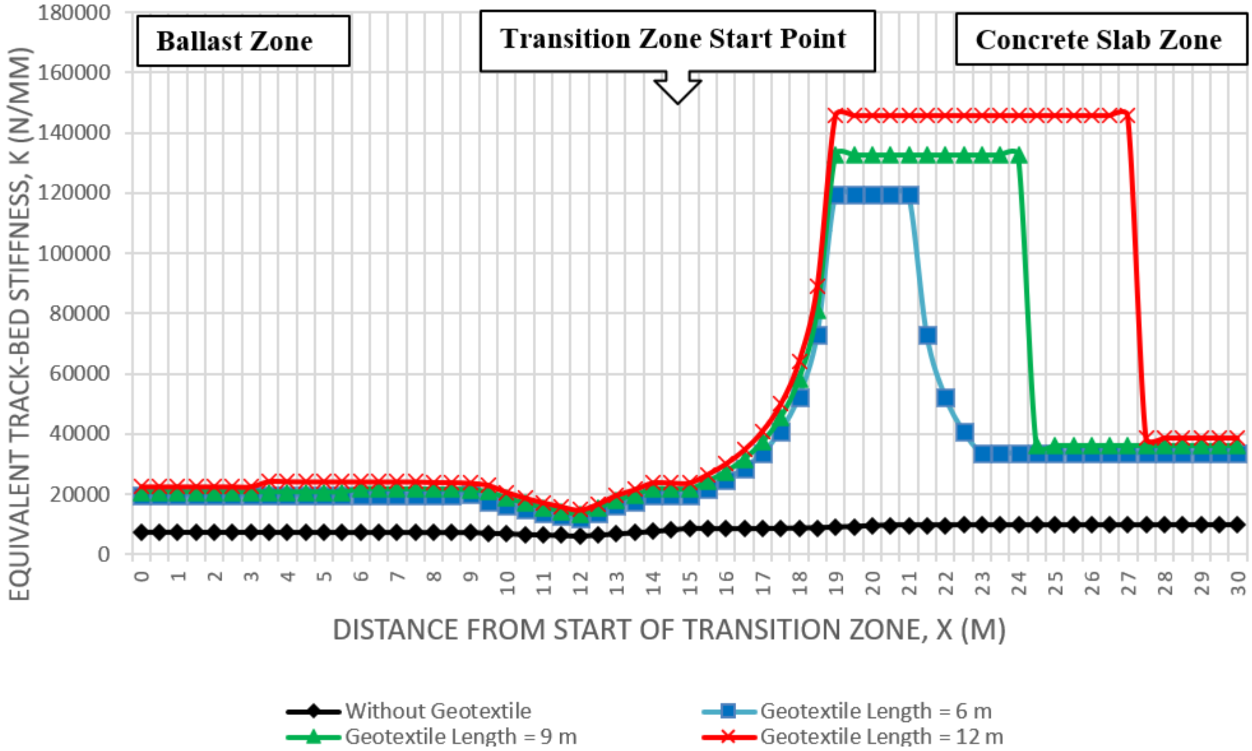

(b)

Fig. 5. Spatial variation of equivalent track-bed stiffness along the slab-ballast transition zone for different geotextile reinforcement lengths (6, 9, and 12 m) under: (a) 160 km/h; and (b) 500 km/h.

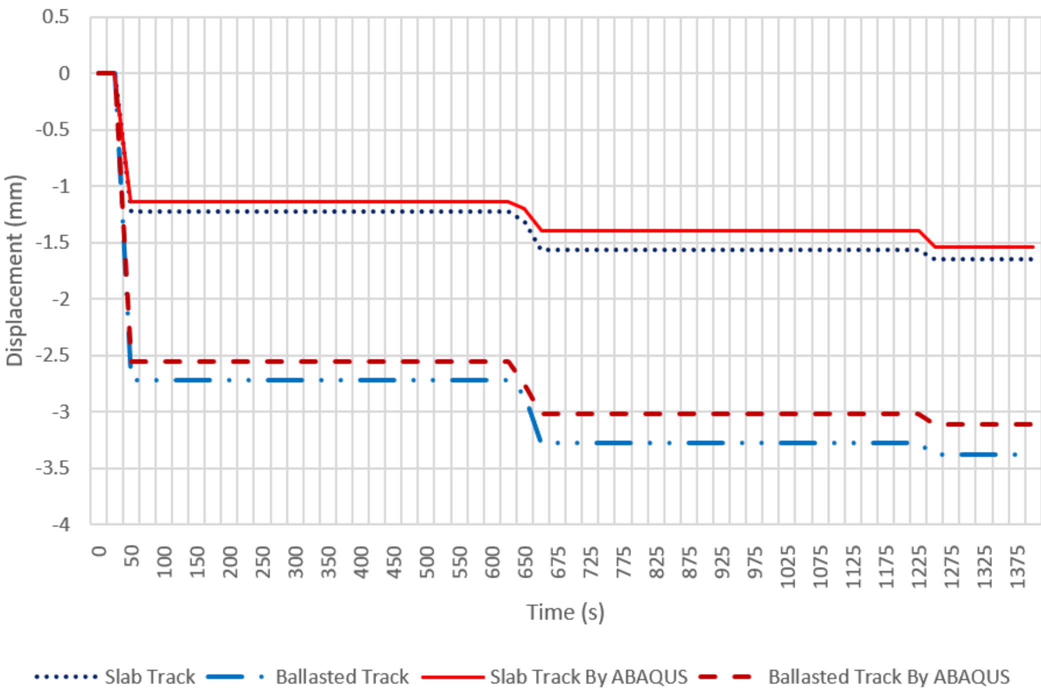

Fig. 6. Validation of the FE model: comparison of average vertical rail displacement between ABAQUS numerical results and experimental data for ballasted and slab track systems.

Table 4. Comparison of mean vertical rail displacements for different track types under static load.

Time (s)	Displacement for slab track (mm)	Displacement for slab track by ABAQUS (mm)	Percentage difference (%)	Displacement for ballasted track (mm)	Displacement for ballasted track by ABAQUS (mm)	Percentage difference (%)
50	-1.223	-1.133	7.36	-2.722	-2.552	6.24
725	-1.315	-1.2	8.74	-2.858	-2.758	3.5
750	-1.567	-1.398	10.78	-3.279	-3.018	7.96
1325	-1.651	-1.537	6.9	-3.376	-3.108	7.94

4. Results and discussion

4.1. Numerical analysis of the transition zone in the absence of a concrete approach slab

The simulation results for the transition zone without a concrete approach slab are presented in Fig. 7. The maximum vertical rail deflection is recorded at approximately 153.18 mm and 180.75 mm for operational speeds of 160 km/h and 500 km/h, respectively. This rapid manifestation of displacement within a short longitudinal distance (less than 6 m) is attributed to the stiffness discontinuity at the ballast-to-slab interface, which induces significant dynamic impact loads on the superstructure. The analysis reveals that the peak vertical displacement occurs 3 meters from the transition onset – a phenomenon governed by the rail's flexural rigidity and the spring-mass modeling of the fastening system – marking the most critical loading state. Based on the analytical framework established in Section 2.6, the calculated track bed stiffness values for the specified speeds are 3,649 N/mm and 6,202 N/mm. These results serve as a baseline for the subsequent parametric study on geotextile integration to optimize track stiffness and minimize vertical oscillations in the transition region.

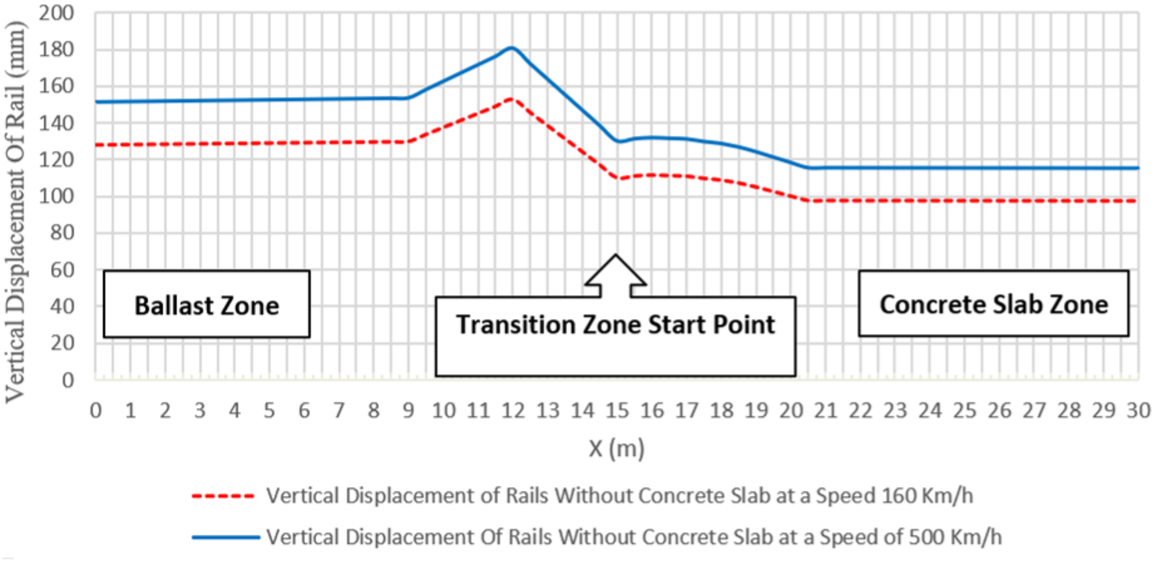

Fig. 7. Vertical rail displacement without a concrete approach slab.

4.2. Effects of train velocity and geotextile reinforcement on transition zone performance

Figs. 8 and 9 present a comparative analysis of vertical rail deflections within the transition zone, specifically investigating the efficacy of a single geotextile layer (as per Section 2.1 specifications) integrated with cement-stabilized ballast and concrete slab sections. At an operational speed of 160 km/h, the implementation of a 6-meter cement-stabilized ballast layer with geotextile results in a vertical rail deflection of approximately 85.15 mm. This deflection is reduced to 76.59 mm and 70.08 mm for 9-meter and 12-meter reinforced zones, respectively. At a higher velocity of 500 km/h, the corresponding deflections are 93.74 mm, 84.17 mm, and 75.55 mm for the 6-, 9-, and 12-meter reinforced sections. These rapid, localized deflections (< 6 m track length) are indicative of significant dynamic loading stemming from the impulsive and transient nature of high-speed train wheel-rail interaction.

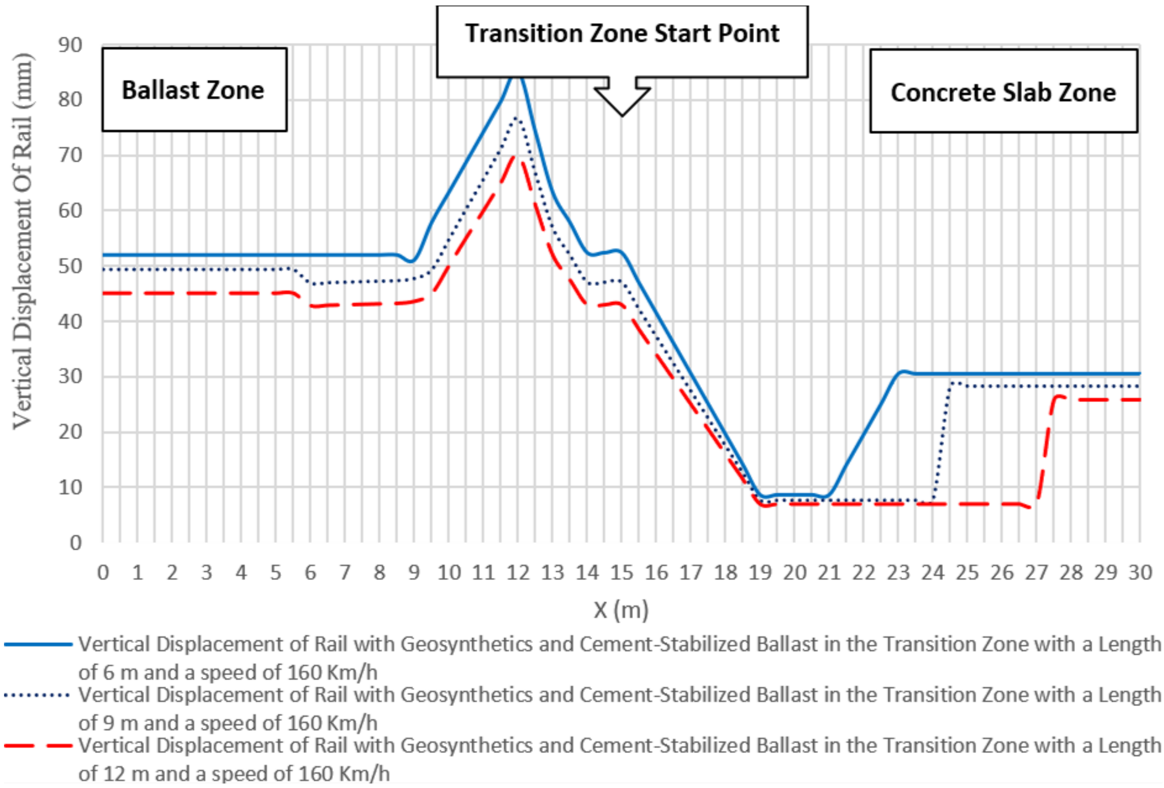

Fig. 8. Vertical rail displacement with cement-stabilized ballast implementation at 160 km/h.

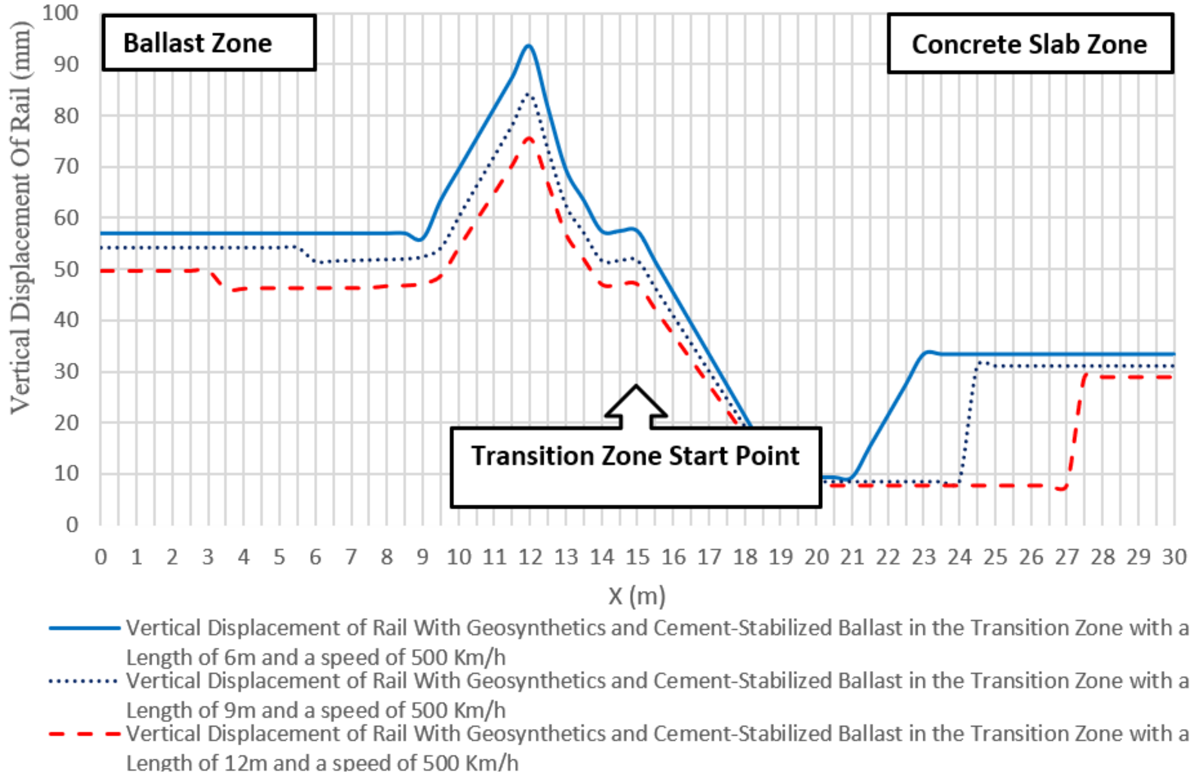

Fig. 9. Vertical rail displacement with cement-stabilized ballast implementation at 500 km/h.

The railbed stiffness for these transition zones, augmented by geotextile, demonstrates a marked increase. For the 160 km/h scenario, stiffness values ascend from 6,565 N/mm (6m) to 7,299 N/mm (9m) and 7,977 N/mm (12m). At 500 km/h, these values escalate substantially to 11,993 N/mm, 13,318 N/mm, and 14,838 N/mm, respectively. The graphical data reveal that the extension of the transition zone by incorporating geotextile – promoting confinement effects within the cement-stabilized ballast and concrete slab, and enhancing their tensile capacity – leads to a notable reduction in vertical rail deflections. At 160 km/h, the percentage reduction in deflection is 44.41%, 50%, and 54.25% for the 6-, 9-, and 12-meter transition lengths, respectively. Correspondingly, at 500 km/h, these reductions are 48.29%, 53.43%, and 58.2%. Notably, the percentage reduction in deflection does not exhibit a commensurate increase with velocity. This observation is ascribed to the inherent transience of high-speed loading; the very short wheel-rail contact duration limits the extent to which higher speeds can amplify the effectiveness of the deflection reduction strategy, even though the absolute deflection values may change.

4.3. Comparative analysis of vertical rail displacement mitigation strategies in transition zones

Table 5 provides a comparative assessment of various strategies for mitigating vertical rail displacement, quantifying the percentage reduction relative to a baseline scenario lacking a concrete approach slab.

Table 5. Comparative analysis of vertical rail displacement mitigation strategies in transition zones.

Transition zone modeling method	Design speed (km/h)	Approach slab length (transition zone, m)	Maximum vertical rail displacement in the transition zone (mm)	Percentage reduction in displacement (%)
Without concrete approach slab	160	—	153.18	—
	500	—	180.75	—
Cement-stabilized ballast	160	6	119.91	21.72
	160	9	110.93	27.59
	160	12	103.67	32.32
	500	6	126.18	30.19
	500	9	116.91	35.32
	500	12	107.79	40.36
Geosynthetic layer on cement-stabilized ballast	160	6	85.15	44.41
	160	9	76.59	50
	160	12	70.08	54.25
	500	6	93.47	48.29
	500	9	84.17	53.43
	500	12	75.55	58.2

In contrast, the implementation of a 12-meter cement-stabilized ballast layer demonstrates significant efficacy, achieving approximately a 40% reduction in vertical rail displacement within the transition zone compared to the unreinforced condition.

However, the optimal strategy identified for minimizing vertical rail deflection in the transition zone is the combined application of a geosynthetic layer atop a 12-meter cement-stabilized ballast section. This integrated approach yields a substantial approximate reduction of 58%, representing the most effective solution investigated.

4.4. Influence of geotextile reinforcement and transition length on vertical rail displacement reduction

Fig. 10 shows that the investigated track stabilization techniques, including cement-stabilized ballast and the combined use of geosynthetics with cement-stabilized ballast, can reduce vertical rail displacement by up to 54% at a constant speed of 160 km/h. This reduction is mainly associated with the improved confinement provided by the geosynthetic-reinforced cement-stabilized ballast layer.

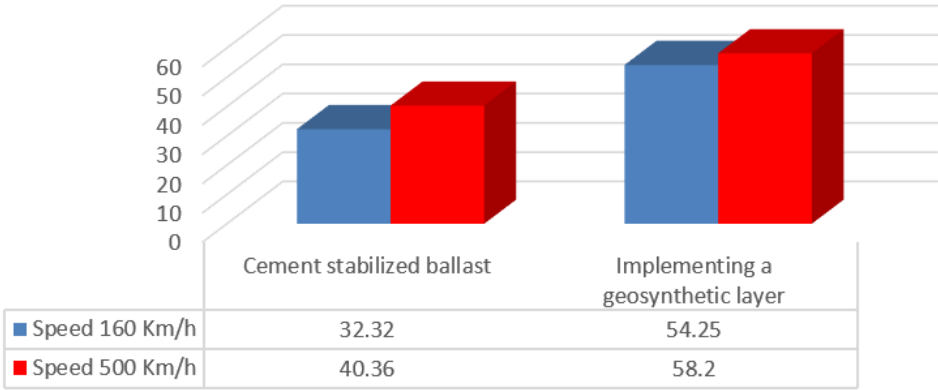

Fig. 10. Maximum percentage reduction in vertical rail displacement at speeds of 160 and 500 km/h.

In addition, extending the pre-slab zone length further decreases vertical rail displacement by approximately 10% in the cement-stabilized ballast case and by about 10% when geosynthetics are incorporated. This beneficial effect is attributed to a wider stress distribution zone and the increased effective anchorage length of the geosynthetic reinforcement.

5. Limitations and future research

The present study employs a dynamic-equivalent loading approach in which train-induced dynamic effects are represented through a Dynamic Impact Factor (DIF). Although this methodology captures the influence of speed-dependent load amplification, several aspects of railway dynamics are not explicitly considered, including moving wheel loads, axle-spacing effects, transient load redistribution, and coupled vehicle-track interaction mechanisms. Consequently, the obtained results should be interpreted within the scope of a simplified engineering assessment of transition-zone performance. Future research should extend the developed numerical framework by incorporating moving-load simulations, vehicle-track-subgrade interaction models, and time-dependent dynamic analyses. Such developments would enable a more comprehensive evaluation of vibration propagation, resonance phenomena, and the long-term behavior of geotextile-reinforced transition zones under realistic operational conditions.

Future validation efforts should extend beyond displacement-based comparisons and include additional response indicators such as stress distribution within ballast layers, permanent settlement evolution, and field-monitoring measurements from operational railway transition zones. Such multi-parameter validation would further enhance confidence in the predictive capability of the proposed numerical framework. Another limitation of the present numerical framework is the assumption of linear elastic behavior for the ballast layer. While this approach enables efficient comparison between different reinforcement configurations, it does not fully represent the nonlinear and path-dependent characteristics of ballast under repeated train loading. More advanced constitutive formulations, such as the Hardening Soil model, Drucker-Prager plasticity model, or Discrete Element Method (DEM)-based approaches, may provide more realistic predictions of ballast degradation, permanent settlement accumulation, and long-term track performance. Future studies should investigate the influence of these advanced material models on the effectiveness of geotextile-reinforced transition zones.

The present study focuses primarily on evaluating the influence of reinforcement length on the performance of railway transition zones, while the mechanical properties of the geotextile were kept constant throughout the analyses. Consequently, the effects of geotextile tensile stiffness, which is recognized as one of the most influential parameters governing reinforcement efficiency, were not explicitly investigated. Variations in tensile stiffness may significantly affect load transfer mechanisms, lateral confinement, membrane action, and the overall deformation response of the track structure. Therefore, the results presented herein should be interpreted within the context of the specific geotextile properties adopted in the numerical model. Future studies should perform comprehensive parametric analyses considering different levels of tensile stiffness (EA), soil-geotextile interface characteristics, ballast stiffness, reinforcement placement depth, and the use of multiple reinforcement layers to establish optimized design recommendations for high-speed railway transition zones.

6. Practical implications

Geotextile reinforcement is expected to enhance track performance and may contribute to reducing maintenance demands by improving the overall structural response of the railway transition zone. However, no explicit economic assessment is carried out in this study. Therefore, any statement regarding cost-effectiveness should be interpreted qualitatively rather than quantitatively. A comprehensive life-cycle cost analysis and maintenance-benefit evaluation are recommended for future research to better quantify the economic implications of the proposed reinforcement approach.

7. Conclusions

The present study investigated the performance of geotextile-reinforced slab-ballast transition zones in high-speed railways using a three-dimensional dynamic-equivalent finite element framework. Based on the obtained results, the following conclusions can be drawn:

- The developed numerical framework successfully quantified the influence of geotextile reinforcement on the mechanical response of railway transition zones and provided a practical methodology for evaluating stiffness-transition improvement strategies.
- Geotextile inclusion within the cement-stabilized ballast layer enhanced the confinement of ballast particles and improved stress redistribution across the slab-ballast interface, resulting in a smoother transition of structural stiffness.
- The results confirmed that train speed remains a dominant factor affecting transition-zone performance. Higher operating speeds increase dynamic load amplification and consequently intensify track deformation, highlighting the need for effective reinforcement measures in future high-speed railway systems.
- Reinforcement length was identified as a key design parameter governing the effectiveness of geotextile stabilization. Extending the reinforcement zone improved load-transfer efficiency and increased the equivalent track-bed stiffness, leading to superior structural performance.
- The combined application of geotextile reinforcement and cement-stabilized ballast demonstrated the most favorable response among the investigated mitigation techniques, indicating its potential as a practical reinforcement strategy for reducing vertical rail displacement and stiffness discontinuities in railway transition zones.
- From an engineering perspective, the proposed reinforcement system may contribute to improved track stability, enhanced serviceability, and reduced maintenance requirements by mitigating excessive deformation at critical slab-ballast interfaces.
- The study contributes to the existing literature by providing one of the first systematic assessments of geotextile reinforcement length in cement-stabilized railway transition zones and by clarifying the underlying confinement mechanisms responsible for performance improvement.
- Despite these findings, the adopted methodology represents a dynamic-equivalent approach and does not explicitly account for moving-load effects, coupled vehicle-track interaction, or ballast material nonlinearity. Future research should therefore incorporate advanced dynamic simulations, field-scale validation, and parametric investigations of geotextile stiffness, interface behavior, and long-term cyclic performance to establish comprehensive design recommendations for next-generation high-speed railway infrastructure.

Statements & declarations

Author contributions

Nima Moslemi Patrudi: Writing - Review & Editing, Visualization, Validation, Software, Resources, Methodology, Investigation, Formal analysis, Data curation, Conceptualization.

Hossein Ghasemzadeh Tehrani: Writing - Review & Editing, Supervision, Methodology, Investigation.

Iman Aghayan: Writing - Review & Editing, Supervision, Methodology, Investigation.

Mohsen Bagheri: Writing - Original Draft, Visualization, Validation, Software, Resources, Methodology, Investigation, Formal analysis, Conceptualization.

Funding

The authors declare that no funds, grants, or other support were received during the preparation of this manuscript.

Data availability

The data that support the findings of this study are available from the corresponding author upon reasonable request.

Declarations

The authors declare that they have no known competing financial interests or personal relationships that could have appeared to influence the work reported in this paper.

References

[1] Shan, Y., Albers, B., Savidis, S. A. Influence of different transition zones on the dynamic response of track–subgrade systems. Computers and Geotechnics, 2013; 48: 21–28. doi:10.1016/j.compgeo.2012.09.006.

[2] Shih, J. Y., Thompson, D. J., Zervos, A. The effect of boundary conditions, model size and damping models in the finite element modelling of a moving load on a track/ground system. Soil Dynamics and Earthquake Engineering, 2016; 89: 12–27. doi:10.1016/j.soildyn.2016.07.004.

[3] Chen, J., Zhou, Y. Dynamic vertical displacement for ballastless track-subgrade system under high-speed train moving loads. Soil Dynamics and Earthquake Engineering, 2020; 129: 105911. doi:10.1016/j.soildyn.2019.105911.

[4] Connolly, D. P., Costa, P. A. Geodynamics of very high speed transport systems. Soil Dynamics and Earthquake Engineering, 2020; 130: 105982. doi:10.1016/j.soildyn.2019.105982.

[5] Zhou, S., Wang, B., Shan, Y. Review of research on high-speed railway subgrade settlement in soft soil area. Railway Engineering Science, 2020; 28: 129–145. doi:10.1007/s40534-020-00214-x.

[6] Charoenwong, C., Connolly, D. P., Colaço, A., Alves Costa, P., Woodward, P. K., Romero, A., Galvín, P. Railway slab vs ballasted track: A comparison of track geometry degradation. Construction and Building Materials, 2023; 378: 131121. doi:10.1016/j.conbuildmat.2023.131121.

[7] Wang, R., Cheng, J.-j., Gao, L., Li, Z.-g., Qi, Y.-l., Wang, M.-t., Ding, B.-s. Research on the swelling mechanism of high-speed railway subgrade and the induced railway heave of ballastless tracks. Transportation Geotechnics, 2021; 27: 100470. doi:10.1016/j.trgeo.2020.100470.

[8] Charoenwong, C., Connolly, D. P., Woodward, P. K., Galvín, P., Alves Costa, P. Analytical forecasting of long-term railway track settlement. Computers and Geotechnics, 2022; 143: 104601. doi:10.1016/j.compgeo.2021.104601.

[9] Coelho, B., Priest, J., Powrie, W., Holscher, P. Monitoring of transition zones in railways. In: 10th international conference and exhibition; 2009 Jun 23–24; London, United Kingdom. p. 1–9.

[10] Sañudo, R., Miranda, M., Markine, V., delÍOlio, L. The Influence of Train Running Direction and Track Supports Position on the Behaviour of Transition Zones. Transportation Research Procedia, 2016; 18: 281–288. doi:10.1016/j.trpro.2016.12.037.

[11] Sadeghi, V., Bagheri, M., Abasi Hamidi, J. Earthquake-Induced Deformation of Road Embankments: A Finite Difference Method. Civil Engineering and Applied Solutions, 2026; 2: 28–41. doi:10.22080/ceas.2026.30800.1066.

[12] Esen, A. F., Woodward, P. K., Laghrouche, O., Čebašek, T. M., Brennan, A. J., Robinson, S., Connolly, D. P. Full-scale laboratory testing of a geosynthetically reinforced soil railway structure. Transportation Geotechnics, 2021; 28: 100526. doi:10.1016/j.trgeo.2021.100526.

[13] Jain, A., Metrikine, A. V., Steenbergen, M. J. M. M., van Dalen, K. N. Railway transition zones: evaluation of existing transition structures and a newly proposed transition structure. International Journal of Rail Transportation, 2024; 12: 979–999. doi:10.1080/23248378.2023.2272668.

[14] Jain, A., Metrikine, A. V., Steenbergen, M. J. M. M., van Dalen, K. N. Dynamic amplifications in railway transition zones: performance evaluation of sleeper configurations using energy criterion. Frontiers in Built Environment, 2024; 10: 1–9. doi:10.3389/fbuil.2024.1285131.

[15] Li, G., Wang, X., Wu, S., li, D., Ma, L., Ding, W. Dynamic response analysis of vehicle-track coupled system at subgrade-bridge transition zone in seasonal frozen region under multi-source excitation. Soil Dynamics and Earthquake Engineering, 2025; 190: 109216. doi:10.1016/j.soildyn.2025.109216.

[16] Cui, W., Xiao, H., Zhong, Y., Ma, C., Gao, L., Chen, H., Zhao, S. Vehicle-induced vibration and damage characteristics of ballastless track in subgrade settlement zone at 400 km/h. Transportation Geotechnics, 2026; 61: 102069. doi:10.1016/j.trgeo.2026.102069.

[17] Tutumluer, E., Kang, M., Qamhia, I. I. A. Geosynthetic stabilization of road pavements, railroads, and airfields. Transportation Geotechnics, 2025; 50: 101321. doi:10.1016/j.trgeo.2024.101321.

[18] Hasheminezhad, A., Ceylan, H., Kim, S., Tutumluer, E. Geosynthetics for resilient geotechnics: A review of applications and innovations. Transportation Geotechnics, 2025; 55: 101676. doi:10.1016/j.trgeo.2025.101676.

[19] Mohan, V., Nandan, A. A comprehensive review of the performance of pine needle geotextiles in reinforced subgrade pavement for sustainable road construction and maintenance. Environmental Science and Pollution Research, 2025; 32: 11838–11878. doi:10.1007/s11356-025-36361-z.

[20] Mohan, V., Nandan, A. Green geotechnical resilient infrastructure: a multi-scale evaluation of pine needle bio-geotextiles to improve land and airfield pavement performance. Innovative Infrastructure Solutions, 2026; 11: 235. doi:10.1007/s41062-026-02651-9.

[21] Petriaev, A., Fedorenko, E. Geosynthetics and Soil Interaction Numerical Modeling for High-speed Rail Lines Substructure. Transportation Research Procedia, 2023; 68: 694–701. doi:10.1016/j.trpro.2023.02.096.

[22] Ahmadi, A., Nasrollahi, K., Nielsen, J. C. O., Dijkstra, J. Dynamic vehicle–track interaction and differential settlement in a transition zone on railway ballast—An integrated 3D discrete–continuum model. Computers and Geotechnics, 2026; 190: 107737. doi:10.1016/j.compgeo.2025.107737.

[23] Punetha, P., Nimbalkar, S. Numerical investigation on dynamic behaviour of critical zones in railway tracks under moving train loads. Transportation Geotechnics, 2023; 41: 101009. doi:10.1016/j.trgeo.2023.101009.

[24] Asghari, K., Sotoudeh, S., Zakeri, J.-A. Numerical evaluation of approach slab influence on transition zone behavior in high-speed railway track. Transportation Geotechnics, 2021; 28: 100519. doi:10.1016/j.trgeo.2021.100519.

[25] Hassan, A. S. M., Khalil, A. A., El-Sonbaty, A. A., Ahmed, H. Y. Comparative numerical study on the performance of different mitigation techniques in high-speed railway transition zones. Soil Dynamics and Earthquake Engineering, 2026; 206: 110256. doi:10.1016/j.soildyn.2026.110256.

[26] Hou, R.-Y., Zheng, J.-J., Fang, H., You, L. An analytical model for dynamic response of geosynthetic reinforced embankment system under traffic load. Computers and Geotechnics, 2022; 142: 104555. doi:10.1016/j.compgeo.2021.104555.

[27] Alam, M. J. I., Gnanendran, C. T., Lo, S. R. Experimental and numerical investigations of the behaviour of footing on geosynthetic reinforced fill slope under cyclic loading. Geotextiles and Geomembranes, 2018; 46: 848–859. doi:10.1016/j.geotexmem.2018.08.001.

[28] Wu, D., Luo, C., Gao, Z., Li, D., Xu, C. Effect of Different Reinforced Load Transfer Platforms on Geosynthetic-Reinforced Pile-Supported Embankment: Centrifuge Model Test. KSCE Journal of Civil Engineering, 2022; 26: 630–649. doi:10.1007/s12205-021-0623-7.

[29] Ding, X., Zhao, J., Ou, Q., Liu, J. Numerical analysis of geosynthetic-reinforced embankment performance under moving loads. Journal of Rock Mechanics and Geotechnical Engineering, 2024; 16: 682–696. doi:10.1016/j.jrmge.2023.04.019.

[30] Liu, K.-F., Feng, W.-Q., Cai, Y.-H., Xu, H., Wu, P.-C. Physical model study of pile type effect on long-term settlement of geosynthetic-reinforced pile-supported embankment under traffic loading. Transportation Geotechnics, 2023; 38: 100923. doi:10.1016/j.trgeo.2022.100923.

[31] Ma, S., Lu, L., Song, A., Wang, Z., Xiao, L., Arai, K. Experimental and Numerical Investigation of Prestressed Geosynthetic-Reinforced Embankment Subjected to Traffic Loading. International Journal of Geomechanics, 2024; 24: 04023250. doi:10.1061/IJGNAI.GMENG-7815.

[32] Hou, R.-Y., Zheng, J.-J., Fang, H., Yang, W.-Y. A Mechanical Model and Solution for Dynamic Response of Geosynthetic-Reinforced Pile-Supported Embankment under Traveling Loads. International Journal of Geomechanics, 2024; 24: 04023260. doi:10.1061/IJGNAI.GMENG-8755.

[33] Alsirawan, R., Alnmr, A., Koch, E. Experimental and Numerical Investigation of Geosynthetic-Reinforced Pile-Supported Embankments for Loose Sandy Soils. Buildings, 2023; 13: 2179.

[34] Zhang, M., Zhu, H., Yang, J., Qiu, C., Javadi, A. A. Experimental study of a 3D printed geogrid embedded with FBG sensor for reinforcement of subgrade with underlying cave. Geotextiles and Geomembranes, 2023; 51: 81–92. doi:10.1016/j.geotexmem.2023.05.001.

[35] Shu, S., Zhang, F., Wang, D., Ge, B., Jiang, Y. Dynamic behavior and characteristics of geogrid-reinforced sand under cyclic loading. Soil Dynamics and Earthquake Engineering, 2024; 180: 108630. doi:10.1016/j.soildyn.2024.108630.

[36] Ghorbanzadeh, A., Nematzadeh, M., Tarkhan, M., Bagheri, M. Experimental and predictive study on shear and electrical behavior of concrete containing ceramic waste and EAF slag after high temperature exposure. Construction and Building Materials, 2026; 536: 146900. doi:10.1016/j.conbuildmat.2026.146900.

[37] Ranjbar, F., Asgari, A., Bagheri, M., Bengar, H. A. Insights into the mechanisms and seismic performance of reinforced concrete buildings on a pile foundation in liquefiable deposits. Structures, 2026; 87: 111557. doi:10.1016/j.istruc.2026.111557.

[38] Forcellini, D., Ranjbar, F., Asgari, A., Bagheri, M., Yazdani, H. Seismic resilience assessment of pile groups against liquefaction-induced lateral spreading: Influence of ground inclination and pile spacing. Engineering Structures, 2026; 360: 122786. doi:10.1016/j.engstruct.2026.122786.